Vol. 12: 29–37, 1999 | CLIMATE RESEARCH Clim Res | Published June 15

Surface conductance and energy exchange in an intensively managed peat pasture

B. O. M. Dirks[1,*], A. Hensen[2]

[1]Wageningen Agricultural University, Dept of Theoretical Production Ecology, PO Box 430, 6700 AK Wageningen, The Netherlands

[2]Netherlands Energy Research Foundation, PO Box 1, 1755 ZG Petten, The Netherlands

ABSTRACT: Aerodynamic measurements of latent (λE) and sensible heat (H) exchange were made in an intensively managed peat pasture during 2 consecutive years; the fetch was approximately 1.5 km. The surface conductance (g_s) was calculated from the Penman-Monteith equation. The analysis focused on 2 successive aspects of g_s: g_s as a function of environment (primarily vapour pressure deficit [D]) and the energy balance as a function of g_s. The effect of D on g_s consisted of 2 components: the range of D over which g_s was reduced (beyond inflection point D_i) and the reducing effect per unit D. As average D increased, so did inflection point D_i and the range of D over which g_s was reduced; the reducing effect per unit D decreased. g_s was a strong mediator in the energy balance. λE increased with D upto the inflection point D_i, beyond which g_s increasingly offset the positive effect of D. As g_s impaired λE, the surface to air temperature difference (ΔT) and consequently H increased. With increasing g_s, λE and H added up to progressively lower values, suggesting an increasing soil heat flux. Hysteresis in the diurnal patterns of the energy balance showed that the positive effect of D on λE remained stronger than the consequent negative effect of g_s. λE was higher after than before noon, whereas ΔT and H were lower.

KEY WORDS: Aerodynamic technique · Surface conductance · Energy exchange · Latent heat · Sensible heat · Pasture · Grassland

1. INTRODUCTION

Surface conductance (g_s) is important in atmospheric-biospheric mass and energy exchange. It is a key factor in canopy CO_2 assimilation and directly determines the latent heat flux (λE), more so than the sensible heat flux (H) and the soil heat flux (G). In the energy balance, g_s is the only biological mediator, whereas the other factors are merely imposed upon the surface.

The effect of g_s and environment on λE varies widely among vegetation types and environmental conditions (Baldocchi 1994). Hiyama et al. (1995) found a substantial divergence in net irradiance (R_n), λE, H and G for different surface types. Jarvis & McNaughton (1986) showed that the impact of g_s on λE depends on the ratio between g_s and aerodynamic conductance (g_a) as a result of the feedback of the canopy's microclimate on λE.

*E-mail: bjorn.dirks@altavista.com

Changes in g_s and λE are reflected in the Bowen ratio ($\beta = H/\lambda E$). Reduced λE as a result of changes in g_s leads to higher surface temperatures. The temperature difference between the surface and air in turn determines both λE and H. Simulation studies have shown that β has a pronounced effect on the development of mesoscale circulations in the atmospheric boundary layer (Segal et al. 1988, Avissar & Pielke 1991, Mascart et al. 1991) — primarily through a differential distribution of H over the land surface.

g_s is generally derived from measurements of the λE. The best established component of g_s is stomatal conductance, which is affected by a number of factors: CO_2 assimilation (Collatz et al. 1991), irradiance and temperature (Avissar et al. 1985, Lindroth & Halldin 1986, Baldocchi et al. 1991), vapour pressure deficit (Price & Black 1990, Leuning 1995, Verhoef et al. 1996), relative air humidity (Collatz et al. 1991), leaf water potential (Lynn & Carlson 1990), λE (Mott & Parkhurst 1991), and soil moisture.

This paper reports on micrometeorological energy flux measurements in intensively managed peat pasture made during 2 consecutive years. Since g_s is the most uncertain factor in the energy balance, the analysis largely focuses on g_s. The analysis has 2 successive objectives: firstly, it determines how g_s was influenced by physical environmental variables; secondly, it demonstrates how g_s determines λE and how this interacted with the dynamics of the energy balance as a whole.

2. MATERIALS AND METHODS

2.1. Experimental site. Measurements were made at the experimental site of the Royal Netherlands Meteorological Institute (KNMI) near Cabauw in The Netherlands (51° 58' N, 4° 55' E). It was surrounded by pasture, orchards, minor roads and a built-up area. The soil consisted of a 0.6 to 0.8 m thick layer of alluvial clay on top of a massive peat layer. The land was composed of long strips alternated by waterways (every 50 m, approximately 5% of the total surface). The vertical distance between land and waterway surface amounted to approximately 0.8 m. The pasture predominantly consisted of *Lolium perenne* and was used for intensive dairy farming (2.5 head of cattle ha^{-1}), with mixed grazing and mowing.

2.2. Flux measurements. Micrometeorological energy exchange measurements were made by the Netherlands Energy Research Foundation (ECN) by applying the aerodynamic gradient technique (Hensen et al. 1997). The measurements covered most of the periods March 1993 up to February 1994 ('1993'), and March 1994 up to February 1995 ('1994').

The aerodynamic gradient technique used wind speed measured at 10 m height. It was determined with an accuracy of 1% using a Gill propeller vane type 8002dx, modified by KNMI. Temperature measurements were obtained at 0.6, 2 and 10 m height; thermocouples measured the direct differences between the successive levels. At 0 m height the thermocouples were measured against a 0°C ice bath. The thermocouples were shielded and ventilated; the accuracy of the temperature differences was approximately 0.05°C. Air humidity followed from air temperature and wet bulb temperature; the set-up for the latter measurement was similar to that of air temperature, but the sensor was kept wet using peristaltic pumps.

Values for the following variables were clustered to 30 min averages: λE (W m^{-2}); H (W m^{-2}); wind speed at 10 m height (u_{10}; m s^{-1}); air temperature at 0.6 m height (T_a; °C); specific air humidity at 0.6 m height (q; g kg^{-1}); vapour pressure deficit at 0.6 m height ($D_{0.6}$; kPa).

2.3. Meteorological measurements. Meteorological measurements and data processing were made by KNMI. Short-wave irradiance (0.3 to 3 µm) was measured using a Kipp CM11 pyranometer, ventilated to prevent condensation on the dome; for diffuse irradiance the pyranometer was equipped with a shadow band. Long-wave irradiance (3 to 50 µm) was measured using a ventilated Eppley radiometer. Measurement of net radiation (0.3 to 50 µm) was made using a Funk radiometer. G was measured using flux plates developed by the TNO Institute of Applied Physics: 3 heat flux plates, 3 m apart, at 0, 5 and 10 cm depth. Values for the following variables were clustered to 30 min averages (W m^{-2}): short-wave irradiance (R_s), diffuse short-wave irradiance, outgoing long-wave radiation (L_{out}), net radiation (R_n), and G. The surface temperature (T_s; °C) was calculated using the Stefan-Boltzmann Law and L_{out}. A surface emissivity of 0.975 was assumed (Ripley & Redmann 1976). The surface to air temperature difference was calculated thus: $\Delta T = T_s - T_a$. Though ΔT holds many uncertainties, it was assumed to be indicative of the actual surface to air temperature difference.

2.4. Analysis of measurements. Only measurements made while the wind direction was between 195° and 250° were analysed. In this range the fetch exclusively consisted of pasture over a distance of 1.5 to 2 km. By restricting the analysis to measurements made during westerly winds, an implicit selection for climate type was introduced. Table 1 shows significant ($p < 0.10$) climatic differences between the 1° to 360° and 195° to 250° ranges. More clouds and precipitation and lower irradiance and temperature extremes indicate that we considered a climate that was slightly more maritime than the actual average. The aerodynamic technique also excluded measurements under wind-still conditions.

Table 1. Average, minimum and maximum values of environmental variables measured while the wind direction was between 1° and 360° and between 195° and 250° near Cabauw, The Netherlands, from March 1993 up to February 1995. All differences between the variables in the 2 ranges were significant ($p < 0.10$)

	1°–360°			195°–250°		
	Avg.	Min.	Max.	Avg.	Min.	Max.
Air temperature (°C)	9.8	–8.2	32.6	9.9	–6.8	25.7
Short-wave irradiance (W m^{-2})	115	–	985	94	–	954
Diffuse fraction	0.68	–	–	0.80	–	–
Air humidity (g kg^{-1})	6.74	–	–	6.87	–	–
Precipitation (mm $\frac{1}{2}h^{-1}$)	0.049	–	–	0.058	–	–

The fluxes were an average of the different states within the fetch of 1.5 km. An increasingly delayed regrowth of grass as the season progresses results in a gradually decreasing average leaf area. Leaf area and leaf characteristics (morphology, physiological response and stomatal conductance; Davies 1988) both affect g_s (Mascart et al. 1991, Saugier & Katerji 1991, Kelliher et al. 1995). Measurements were generally analysed at a monthly time scale. A distinction was made between daytime and nighttime measurements.

Linear regression was done by the least squares technique; non-linear regression analysis followed the iterative Marquardt-Levenberg algorithm (Fox et al. 1994).

2.5. Closure of energy balance. In the pasture's energy balance, both advection and biochemical and physical energy storage were neglected. Fig. 1 shows a close correspondence of the energy available for upward dissipation ($R_{in} = R_n - G$) and actual upwardly dissipated energy ($R_{out} = \lambda E + H$), despite the different spatial scales for the components (H and λE, 1 km^2; R_n and G, 1 m^2). No significant difference between R_{in} and R_{out} was observed during either year.

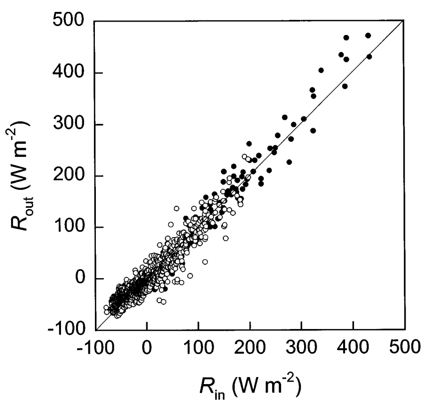

Fig. 1. Energy balance for the pasture near Cabauw, The Netherlands, in 1993 (●) and 1994 (○): comparison of available energy ($R_{in} = R_n - G$) and outgoing energy ($R_{out} = \lambda E + H$) in the wind direction 195°–250°. R_n: net radiation; G: soil heat flux; λE: latent heat flux; H: sensible heat flux

2.6. Latent heat flux and surface conductance. Key to the surface energy balance is the relation between g_s and λE. g_s is the mediating (surface) factor that operates in a system of otherwise external (aerial and radiative) factors. g_s as such cannot be measured but is derived from measurements of λE. In the analysis of the dynamics of the energy balance, 3 successive stages were distinguished: (1) the relationship between g_s and environmental factors; (2) the relationship between λE and g_s; and (3) the relationship between β, λE and g_s. As for now, the first two will be considered.

Two relationships that relate the λE to environmental and surface factors were applied. The latent heat loss equation was used for the analysis of the dynamics of λE. The Penman-Monteith equation was used to calculate g_s that was subsequently analysed in relation to environmental factors.

The latent heat loss equation causally relates λE to environmental and surface factors (Monteith & Unsworth 1990):

$$\lambda E = (0.622\lambda \rho_a/p)(D + s\Delta T)/(r_a + r_s) \qquad (1a)$$

where ρ_a is the density of the dry air (g m^{-3}), p the air pressure (kPa), D the aerial vapour pressure deficit (kPa), ΔT the difference between T_s and T_a (°C), s the slope of the saturation vapour pressure curve at T_a (kPa K^{-1}), r_a and r_s the aerodynamic and surface resistances to water vapour transfer (s m^{-1}), and λ the latent heat of vaporisation (J g^{-1}). Eq. (1a) was used for the analysis of the dynamics of λE only, because of the uncertainty in the application of ΔT.

The Penman-Monteith equation is derived from Eq. (1a) and mathematically rather than causally relates λE to environmental and surface factors (Monteith & Unsworth 1990):

$$\lambda E = [s(R_n - G) + \rho_a c_p D/r_a]/[s + \gamma(r_a + r_s)/r_a] \qquad (1b)$$

where γ is the psychrometer constant (kPa K^{-1}); and c_p the specific heat of air at constant pressure (J g^{-1} K^{-1}). Aerodynamic conductance, g_a, was calculated as $(u_{0.6}/u_*^2 + 5.31u_*^{-2/3})^{-1}$ (Thom 1972, 1975, Verma et al. 1986, Monteith & Unsworth 1990, Lhomme 1991, Saugier & Katerji 1991), where u_* is the friction velocity (m s^{-1}). $u_{0.6}$ was calculated from the logarithmic wind profile, with $u_* = 0.141u_{10}$, zero plane displacement = 0.05 m, and roughness length, z_0 = 0.021 to 0.066 m.

Calculation of g_s from Eq. (1b) involves several variables. A comparison was made between g_s that includes all these variables and g_s that assumes constants for several of these variables: G (0 W m^{-2}), p (101 kPa), γ (0.066 kPa K^{-1}), λ (2477 J g^{-1}), ρ_a (1246 g m^{-3}) and z_0 (0.03 m). The 2 conductances did not differ significantly. Fig. 2 compares the values of total conductance to water vapour transfer, $g = (g_a + g_s)/(g_a \times g_s)$, calculated with and without the assumption of constants. We used the g_s calculated with the assumed constants.

2.7. Surface conductance and environment. g_s is correlated with CO_2 assimilation, but is also influenced by vapour pressure. A multiplicative relationship was used to analyse the surface conductance as a function of R_s and surface vapour pressure deficit (D_0). A rectangular hyperbolic relationship between R_s and g_s

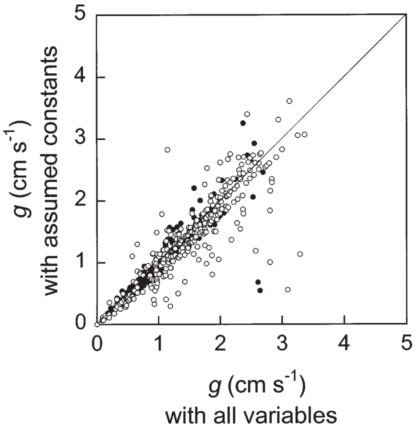

Fig. 2. Comparison of daytime conductance to water vapour transfer *(g)* with and without several variables assumed constant in 1993 (●) and 1994 (○)

which is characterised by $g_{s,mx}$ as the maximum surface conductance was assumed (Kelliher et al. 1995, Schulze et al. 1995).

Three different relationships between D_0 and g_s were evaluated: (a) linear; (b) negatively exponential (Jones 1992); and (c) hyperbolic (Leuning 1995, Schulze et al. 1995):

$$f(D_0) = 1 - (D_0 - D_i)/d_{lin} \quad (2a)$$

$$f(D_0) = e^{-(D_0 - D_i)/d_{exp}} \quad (2b)$$

$$f(D_0) = [1 + (D_0 - D_i)/d_{hyp}]^{-1} \quad (2c)$$

where $f(D_0)$ is the relative effect of D_0 on g_s, D_i is the vapour pressure deficit inflection point with $f(D_0) = 1$ for $D_0 < D_i$, and d_{lin}, d_{exp} and d_{hyp} are equation-specific parameters.

Table 2. Explained variance (r^2) and fitted parameters ($p < 0.10$) for surface conductance (g_s) as a hyperbolic function of short-wave irradiance (R_s) and an exponential function of vapour pressure deficit (D_0) in the wind direction range 195°–250°; λE and $\lambda E_{eq} > 0$ W m^{-2}; $\Omega < 0.70$. $D_{0.6}$: vapour pressure deficit at 0.6 m (p_{95}: 95 percentile). $g_{s,mx}$: maximum surface conductance; d_{exp}: parameter of exponential relationship; D_i: vapour pressure deficit inflection point. n: number of observations

	$D_{0.6}$ (p_{95}) (kPa)	$g_s = f(R_s)$ n	r^2	$g_s = f(R_s, D_0)$ r^2	$g_{s,mx}$ (cm s^{-1})	d_{exp} (kPa)	D_i (kPa)
Apr 1993	0.79	47	0.04	0.56		0.51	
Jun 1993	1.39	42	0.04	0.50	3.0	0.78	0.21
Jul 1993	1.05	204	0.08	0.27	2.3	0.57	0.60
Aug 1993	0.98	141	0.40	0.52	2.7	1.11	0.64
Sep 1993	0.71	58	0.11	0.38	5.1	0.63	0.24
Apr 1994	0.84	94	0.04	0.23	3.4	0.38	0.34
May 1994	0.63	39	0.33	0.35	2.6		
Aug 1994	1.16	106	0.02	0.38	1.8	0.72	0.40
Oct 1994	0.58	31	0.56	0.77	6.9	0.46	
Jan 1995	0.41	70	0.06	0.18	4.5		0.27

For this analysis, situations with wet surfaces were excluded by only considering values of the λE and equilibrium latent heat flux (λE_{eq}) > 0 W m^{-2}. λE_{eq} is λE in a situation where the g_a approaches 0; it equals $s \times R_n/(s + \gamma)$ (Jones 1992). s is the slope of the saturation vapour pressure curve at T_a (kPa K^{-1}). Situations with a low degree of coupling between the atmosphere and surface (Jarvis & McNaughton 1986) were excluded by only considering values where the decoupling coefficient (Ω) < 0.70 [$\Omega = (s/\gamma + 1)(s/\gamma + 1 + g_a/g_s)^{-1}$]. D_0 was calculated from $D_{0.6}$, g_a, λE and λE_{eq} as described by Kelliher et al. (1993).

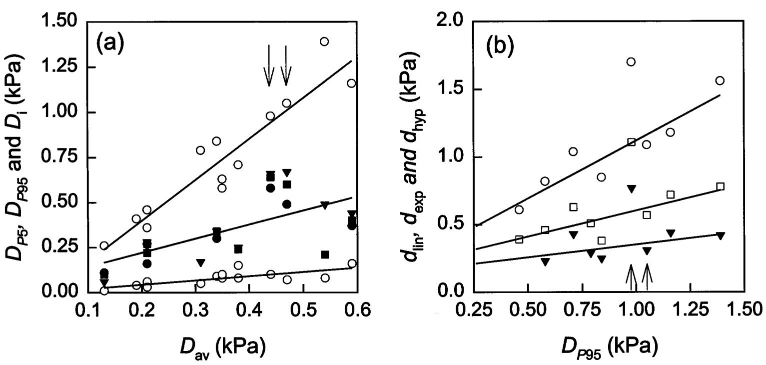

Fig. 3. (a) Monthly p_5 and p_{95} (5 and 95 percentiles) of vapour pressure deficit *(D*; ○), monthly fitted (●, ■ and ▼ from Eqs. 2a, 2b & 2c, respectively) and regressed (—) inflection point D_i as a function of average vapour pressure deficit (D_{av}). (b) Monthly fitted and regressed d_{lin} (○), d_{exp} (□) and d_{hyp} (▼) as a function of the p_{95} of vapour pressure deficit (D_{p95}). Arrows: July and August 1993

3. RESULTS

3.1. Surface conductance

The fitted $g_{s,mx}$ at non-limiting irradiance and vapour pressure deficit ranged from 3–5 cm s^{-1} in spring and 2–3 cm s^{-1} in summer to 5–7 cm s^{-1} in autumn (Table 2).

D was a major reducing factor of g_s (Table 2). In increasing the explained variance, the exponential equation for the effect of D was slightly more effective than the hyperbolic and linear equations. Eqs. (2b) & (2c) altogether provided the best description for the effect of D on g_s, but differences were minor.

Fig. 3a shows a positive relationship between monthly average vapour pressure deficit (D_{av}) and monthly fitted D_i (the value of D_0 beyond which g_s is progressively reduced). The range of D over which g_s was reduced (D_i to D_{p95}) increased with D_{av}. July and August 1993 deviated from this trend: D_i to D_{p95} was smaller than expected.

Fig. 3b shows that monthly fitted parameters d_{lin}, d_{exp} and d_{hyp} from Eqs. (2a), (2b) & (2c) were positively related to D. In other words, the larger range of D over which g_s was reduced (D_i to D_{p95}), the smaller the reduction per unit D.

3.2. Soil heat flux

An upward G of 3 W m^{-2} was fitted for zero R_n in 1993. Fig. 4 shows that the gradient of daytime G against R_n was 0.1 (r^2 = 0.56, n = 962).

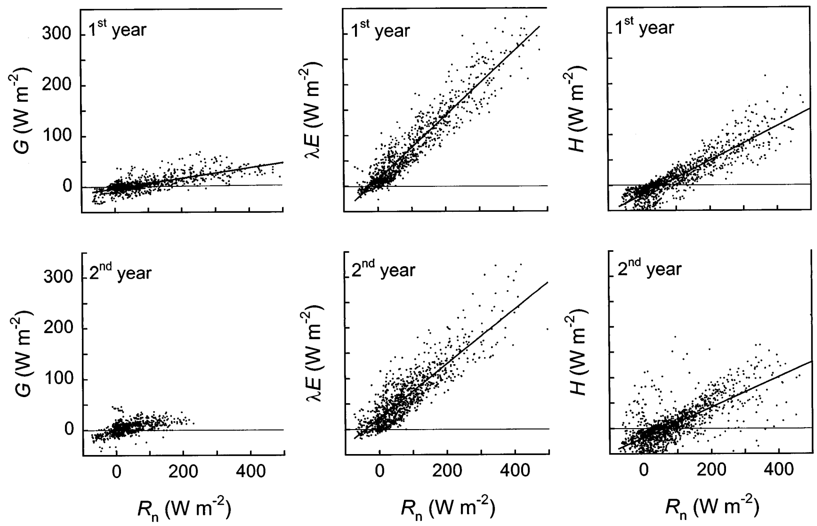

Fig. 4. Daytime soil heat flux (G), latent heat flux (λE), and sensible heat flux (H) as a function of net irradiance (R_n) in the wind direction 195°–250° in 1993 and 1994

3.3. Latent heat flux

Fig. 4 shows that the gradient of daytime λE against R_n was 0.55 to 0.65 ($b_{\lambda E}$) on a yearly basis. $b_{\lambda E}$ differed significantly between 1993 and 1994 ($p < 0.001$).

In spring and summer, $b_{\lambda E}$ ranged from 0.52 to 0.70 (Table 3). The highest value of $b_{\lambda E}$ was fitted for August 1993; at this time high levels of D and g_s at moderate levels of ΔT occurred. Low values of $b_{\lambda E}$ fitted for June 1993 and August 1994 are associated with high levels of D and ΔT and low levels of g_s. The period June to August 1993 was characterised by drought and sustained high levels of D, but progressively higher values of g_s and lower values of ΔT; $b_{\lambda E}$ increased over this period.

Different degrees of dissipation of daytime R_n into λE were observed when distinguishing between different g_s classes (Fig. 5). The regression coefficients in Table 4 (intercept $a_{\lambda E}$ and slope $b_{\lambda E}$) show that this dissipation of R_n was reduced at decreased g_s.

3.4. Sensible heat flux

Fig. 4 shows that the gradient of daytime H against R_n was 0.30 to 0.35 (b_H) on a yearly basis. b_H differed significantly between 1993 and 1994 ($p < 0.01$).

Table 3. Explained variance (r^2) and regression coefficients ($p < 0.10$) for daytime latent heat flux (λE) and sensible heat flux (H) as a linear function of the net irradiance (R_n) in the wind direction range 195°–250°. a: intercept; b: slope. R_n > 100 W m^{-2}. $D_{0.6}$: vapour pressure deficit at 0.6 m; ΔT: surface to air temperature difference; g_s: surface conductance; n: number of observations

	$p_5 - p_{95}$				$\lambda E = f(R_n)$ (W m^{-2})				$H = f(R_n)$ (W m^{-2})			
	$D_{0.6}$ (kPa)	ΔT (°C)	g_s (cm s^{-1})	n	$a_{\lambda E}$	$b_{\lambda E}$	r^2	n	a_H	b_H	r^2	n
Apr 1993	0.1–0.8	0.2–5.7	1.3–3.8	31	12	0.62	0.95	66	–19	0.31	0.78	116
Jun 1993	0.2–1.4	0.3–6.0	0.4–2.8	30	18	0.55	0.94	70	–18	0.36	0.90	74
Jul 1993	0.2–1.1	1.1–4.9	0.6–3.7	146	12	0.62	0.87	283	–12	0.36	0.84	292
Aug 1993	0.2–1.4	0.1–5.6	0.9–3.6	93	12	0.70	0.90	178	–15	0.27	0.81	188
Sep 1993	0.1–0.7	0.6–4.1	1.0–4.7	45	14	0.66	0.87	69	–19	0.35	0.86	74
Apr 1994	0.1–0.9	0.4–5.8	0.9–6.5	61	25	0.52	0.76	127	–18	0.31	0.73	161
May 1994	0.2–0.7	0.4–3.0	1.4–2.9	37	15	0.63	0.89	48	5	0.23	0.03	52
Aug 1994	0.3–1.2	0.7–8.5	0.4–2.2	74	16	0.52	0.83	138	–19	0.39	0.90	144
Sep 1994	0.2–0.7	0.6–2.7	0.8–4.2	41	10	0.68	0.85	99	–21	0.32	0.83	111
Oct 1994	0.3–0.6	1.0–4.6	1.4–3.0	16	22	0.55	0.78	87	–21	0.38	0.86	91
Feb 1995	0.2–0.4	0.0–1.4	1.6–3.8	55	28	0.53	0.63	217	–34	0.37	0.65	222

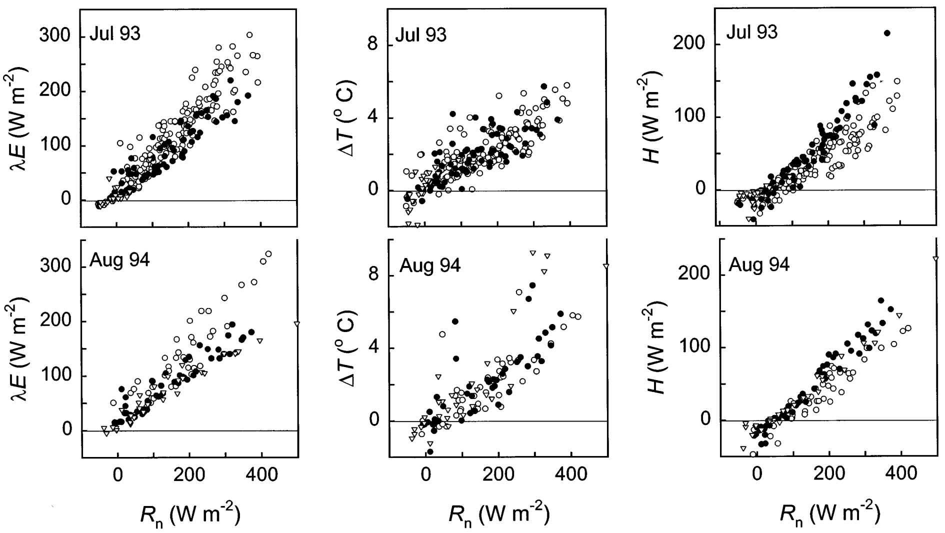

Fig. 5. Daytime latent heat flux (λE), sensible heat flux (H), and surface to air temperature difference (ΔT) as a function of net irradiance (R_n) in the wind direction 195°–250° in July 1993 and August 1994 for the following surface conductance (g_s) classes: >1.0 (○), 0.5–1.0 (●), and <0.5 cm s^{-1} (▽)

In spring and summer, b_H ranged from 0.23 to 0.39 (Table 3). The lowest value of b_H was fitted for August 1993 at the same time as the highest value of $b_{\lambda E}$. ΔT was lowest in August 1993. High values of b_H were fitted for June and July 1993 and August 1994, generally months with lower values of $b_{\lambda E}$. Levels of ΔT were relatively high in these months.

Different degrees of dissipation of daytime R_n into H were observed when distinguishing between different g_s classes (Fig. 5). The regression coefficients in Table 4 (a_H and b_H) show that the dissipation of R_n into H increased with decreasing g_s from the highest to the middle g_s class, but remained approximately constant in the transition from the middle to the lowest g_s class. Table 4 also shows that the increase in ΔT with increasing R_n ($b_{\Delta T}$) generally remained constant with decreasing g_s (Fig. 5). In August 1994, $b_{\Delta T}$ increased and g_a decreased in the transition from the middle to the lowest g_s class.

Table 4. Average aerodynamic conductance (g_a) and regression coefficients ($p < 0.10$) for daytime latent heat flux (λE), sensible heat flux (H) and surface to air temperature difference (ΔT) as a linear function of net irradiance for different surface conductance (g_s) classes in the wind direction range 195°–250° in July 1993 and August 1994. *a*: intercept; *b*: slope. Superscripts indicate within-month differences ($p < 0.10$)

Parameter	g_s (cm s^{-1})				
	July 1993		August 1994		
	>1.0	0.5–1.0	>1.0	0.5–1.0	<0.5
g_a (cm s^{-1})	3.6^a	3.2^a	3.0^a	3.1^a	2.2^b
$a_{\lambda E}$ (W m^{-2})	16^a	14^a		19^a	17^a
$b_{\lambda E}$	0.66^a	0.51^b	0.68^a	0.44^b	0.39^b
a_H (W m^{-2})	−16^a	−20^a	−26^a	−25^a	−16^b
b_H	0.33^a	0.49^b	0.36^a	0.47^b	0.41^b
$a_{\Delta T}$ (°C)	0.5^a	0.4^a			
$b_{\Delta T}$ [°C (W m^{-2})$^{-1}$]	0.010^a	0.011^a	0.014^a	0.015^a	0.022^b

Fig. 6 illustrates the approximately linear relationship between the independently determined ΔT and H in 1993. The slope was 24 W m^{-2} (°C)$^{-1}$ in 1993 (r^2 = 0.76, n = 2105) and 21 W m^{-2} (°C)$^{-1}$ in 1994 (r^2 = 0.59, n = 2701). The regression coefficients differed significantly ($p < 0.001$).

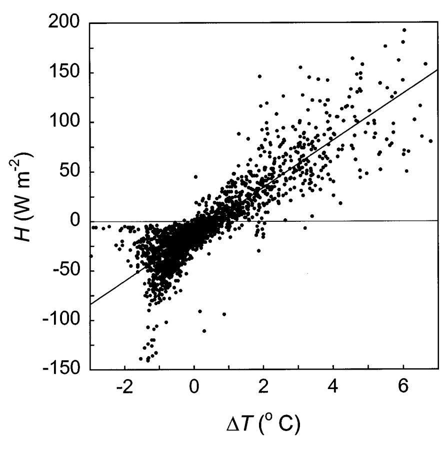

Fig. 6. Sensible heat flux (H) as a function of surface to air temperature difference (ΔT) in the wind direction 195°–250° in 1993

3.5. Diurnal patterns and hysteresis

λE, H, D, ΔT and g_s were clustered to monthly average diurnal patterns. Before and after noon responses of these variables to R_n were compared (Fig. 7).

g_s after noon was generally lower than g_s before noon; levels of g_s were lower in August 1994 than in August 1993. λE followed the pattern of D, though less pronounced; the difference before and after noon was

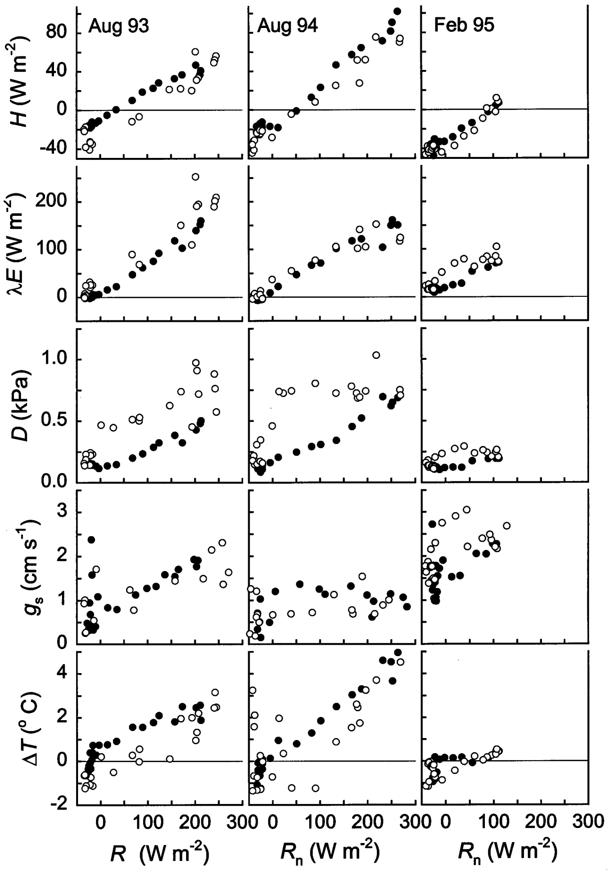

Fig. 7. Average diurnal response to net irradiance (R_n) of the sensible heat flux *(H)*, latent heat flux *(λE)*, vapour pressure deficit *(D)*, surface conductance *(g_s)* and surface to air temperature difference (Δ*T)* before (●) and after noon (○) in the wind direction 195°–250° in August 1993, August 1994 and February 1995. For each 30 min average n ≥ 3

lowest in August 1994. Δ*T* after noon was lower than before noon. *H* followed the pattern of Δ*T*.

4. DISCUSSION

4.1. Surface conductance

Saugier & Katerji (1991) and Kelliher et al. (1995) found $g_{s,mx}$ to range from 0.9–1.7 cm s^{-1} in natural grassland to 3.3–5.0 cm s^{-1} in crops, covering the annual range found in this study. Kelliher et al. (1995) noted that fitted $g_{s,mx}$ values tend to be approximately 25% higher than observed $g_{s,mx}$ values.

$g_{s,mx}$ as such is theoretical, since irradiance and vapour pressure deficit are positively correlated. However, the annual pattern of $g_{s,mx}$ is indicative of stable pasture characteristics. Leaf area is reflected in the long-term patterns of $g_{s,mx}$: high after the first period of regrowth in early spring, gradually decreasing towards late autumn. This could explain most of the observed pattern of $g_{s,mx}$.

Values of $g_{s,mx}$ were generally speculative for autumn, since these values were never actually reached. The close relationship (Collatz et al. 1991, Leuning 1995) between CO_2 assimilation and g_s suggests that g_s at lower irradiance may have been limited by temperature, more so in autumn than in spring or summer. This could have resulted in a reduced initial response of g_s to irradiance and the apparently high $g_{s,mx}$.

Stomatal conductance in grass has been shown to be particularly sensitive to *D* (Woledge et al. 1989). Fitted parameters d_{lin}, d_{exp} and d_{hyp} suggest effects that were stronger than found in cereals (0.40 kPa^{-1}; Kim et al. 1989). The exponential and hyperbolic equations for the description of the effect of *D* on g_s were slightly more effective than the linear equation.

The effect of *D* on g_s consisted of 2 components: (1) the range over which *D* is effective (D_i to D_{p95}) and (2) the reducing effect on g_s per unit *D* (through d_{lin}, d_{exp} and d_{hyp}). Fig. 3 shows that an increasing *D* resulted in an increase of the D_i to D_{p95} range, despite an upward shift of D_i. An increased *D* simultaneously resulted in a decrease in the effect on g_s per unit *D*. This suggests that the instantaneous response of the vegetation's surface to *D* was an adaptation to average levels of *D*. The reducing effect of *D* on g_s was maintained and remained distributed over most of the actual *D* range. Stomatal adjustment (Drake & Salisbury 1972) traded off between g_s for sustained CO_2 assimilation and reduced transpiration over the full range of irradiance.

The surface response deviated from this trend in July and August 1993. Both the range over which *D* affected g_s and the effect on g_s per unit *D* were lower than expected. The period from June to August 1993 was characterised by progressively lower levels of *D*. It suggests an adaptation of g_s to *D* extending beyond the time frame of 1 mo.

The effects of soil moisture and *D* on g_s may have been confounded. However, in August 1994, a severe reduction in canopy CO_2 assimilation and growth in a non-irrigated pasture on alluvial clay, 50 km east of the site, was largely removed by lowering *D* (authors' unpubl. results).

4.2. Soil heat flux

A 10% dissipation of R_n into *G* is modest. Kim & Verma (1990) found 10 to 25% in a tallgrass prairie, where the variation was attributed to differences in surface cover and soil moisture. In temperate pastures, surface cover and soil moisture are generally high and stable relative to R_n throughout much of the year.

4.3. Latent heat flux

The effect of D and ΔT on λE was mediated by g_s. D had a direct positive effect on λE, but beyond D_i it simultaneously had a negative effect on g_s—thus an indirect negative effect on λE. The direct and indirect effects of D increasingly offset each other. Jarvis (1981) found this moderation of the effect of D (from 1.5 kPa) by g_s in Scots pine.

The mediating effect of g_s on the effect of D was best observed in June 1993 and August 1994 (low g_s) and August 1993 (high g_s). At sustained high levels of D, λE increased less with R_n at lower levels of g_s, illustrated by low $b_{\lambda E}$. Reduced λE co-occurred with an increased ΔT. August 1993 represented an 'optimum' situation ($b_{\lambda E} \approx 0.70$).

4.4. Sensible heat flux

A low g_s at high levels of D reduced the λE and increased ΔT. g_a and ΔT constitute the main causal factors in H. A reduced λE and increased ΔT in June and July 1993 and August 1994 increased the dissipation of R_n into sensible heat, illustrated by high b_H. August 1993 represented an 'optimum' situation ($b_H \approx 0.25$).

4.5. Bowen ratio

At a constant g_s, Jarvis (1981) found a decreasing β when moving from a maritime to a continental climate. However, a D increasing beyond D_i decreased g_s. This progressively counteracted the increase in λE, increasing H through ΔT. In tallgrass, Kim & Verma (1990) found β to vary between 0.3 (D = 1.8 kPa and g_s = 1.3 cm s^{-1}) and 1.3 (D = 4.3 kPa and g_s = 0.3 cm s^{-1}). Table 4 shows that the dissipation of R_n into λE and H added up to increasingly lower values with decreasing g_s. An increased G may have been the result.

A simple iterative energy balance of a hypothetical leaf (Jones 1992) was calculated. It included Eq. (1a) for λE, the standard equation for H (Monteith & Unsworth 1990) and the Stefan-Boltzmann Law for long-wave irradiance. They suggest that for 'observed' ranges of g_a and g_s, λE is little affected by g_a. A decrease in g_s results in a decrease in λE and an increase in ΔT and H; the sum of λE and H is positively correlated with g_s. Low g_a seriously reduces H and increases ΔT, but in reality a resulting increased buoyancy may again enhance H.

The increase in λE with R_n ($b_{\lambda E}$ in Table 4) was tested against the steady-state theory of Eq. (1b). The increase in ΔT with R_n ($b_{\Delta T}$ in Table 4) was tested against the standard equation for H (Monteith & Unsworth 1990). The covariance of D and R_n was 0.003 kPa (W m^{-2})$^{-1}$, s was 0.15 kPa K^{-1}, g_a and b_H were the values in Table 4, and g_s was 2.0, 0.7 and 0.4 cm s^{-1}. For the 3 g_s classes, Eq. (1b) predicts $b_{\lambda E}$ values of 0.84, 0.51 and 0.40. The standard equation for H predicts $b_{\Delta T}$ values of 0.010, 0.012 and 0.015°C (W m^{-2})$^{-1}$. These predictions are lower than the observations, possibly as a result of reduced λE at the non-irrigated site where ΔT was determined.

4.6. Diurnal patterns and hysteresis

Due to hysteresis, the diurnal pattern of the energy balance gives a more accurate description of its dynamics as compared to the average parameterisation.

D was the main factor in λE, since λE was higher after than before noon, despite a lower g_s. Consequently, ΔT and H after noon were lower than before noon, whereas a sole decrease in g_s would have resulted in the opposite. This was observed for both a normal (1993) and a dry summer month (1994), though the dissipation of R_n into λE was relatively low at drought. Baldocchi et al. (1981) observed simultaneous increases in D and λE and a decrease in downward CO_2 flux in soybean under conditions of heat advection; a decreased g_s may have reduced CO_2 assimilation but the consequence for λE may have been compensated for by D.

Acknowledgements. This study was partly funded by the National Research Programme on Global Air Pollution and Climate Change (project nr. 852062). KNMI provided site facilities and processed the meteorological data. J. Goudriaan and R. Rabbinge commented on the manuscript.

LITERATURE CITED

Avissar R, Pielke RA (1991) The impact of plant stomatal control on mesoscale atmospheric circulations. Agric For Meteorol 54:353–372

Avissar R, Avissar P, Mahrer Y, Bravdo BA (1985) A model to simulate response of plant stomata to environmental conditions. Agric For Meteorol 34:21–29

Baldocchi D (1994) A comparative study of mass and energy exchange over a closed C_3 (wheat) and an open C_4 (corn) canopy: I. The partitioning of available energy into latent and sensible heat exchange. Agric For Meteorol 67: 191–220

Baldocchi DD, Verma SB, Rosenberg NJ (1981) Mass and energy exchanges of a soybean canopy under various environmental regimes. Agron J 73:706–710

Baldocchi DD, Luxmoore RJ, Hatfield JL (1991) Discerning the forest from the trees: an essay on scaling canopy stomatal conductance. Agric For Meteorol 54:197–226

Collatz GJ, Ball JT, Grivet C, Berry JA (1991) Physiological and environmental regulation of stomatal conductance, photosynthesis and transpiration: a model that includes a laminar boundary layer. Agric For Meteorol 54:107–136

Davies A (1988) The regrowth of grass swards. In: Jones MB, Lazenby A (eds) The grass crop — the physiological basis of production. Chapman and Hall, London, p 85–127

Drake BG, Salisbury FB (1972) After effects of low and high temperature pretreatments on leaf resistance, transpiration and leaf temperature in *Xanthium*. Plant Physiol 50: 572–575

Fox E, Kuo J, Tilling L, Ulrich C (1994) SigmaStat user's manual. Jandel Scientific, Erkrath

Hensen A, Van den Bulk WCM, Vermeulen AT, Wyers GP (1997) CO_2 exchange between grassland and the atmosphere — results over a four year period of CO_2 measurements at Cabauw, the Netherlands. Report ECN-C--97-032. Netherlands Energy Research Foundation, Petten

Hiyama T, Sugita M, Kayane I (1995) Variability of surface fluxes within a complex area observed during TABLE 92. Agric For Meteorol 73:189–207

Jarvis PG (1981) Stomatal conductance, gaseous exchange and transpiration. In: Grace J, Ford ED, Jarvis PG (eds) Plants and their atmospheric environment — the 21st Symposium of The British Ecological Society, Edinburgh 1979. Blackwell, Oxford, p 175–204

Jarvis PG, McNaughton KG (1986) Stomatal control of transpiration: scaling up from leaf to region. Adv Ecol Res 15: 1–49

Jones HG (1992) Plants and microclimate, 2nd edn. Cambridge University Press, Cambridge

Kelliher FM, Leuning R, Schulze ED (1993) Evaporation and canopy characteristics of coniferous forests and grasslands. Oecologia 95:153–163

Kelliher FM, Leuning R, Raupach MR, Schulze ED (1995) Maximum conductances for evaporation from global vegetation types. Agric For Meteorol 73:1–16

Kim J, Verma SB (1990) Components of surface energy balance in a temperate grassland ecosystem. Boundary Layer Meteorol 51:401–417

Kim J, Verma SB, Rosenberg NJ (1989) Energy balance and water use of cereal crops. Agric For Meteorol 48:135–147

Leuning R (1995) A critical appraisal of a combined stomatal-photosynthesis model for C_3 plants. Plant Cell Environ 18: 339–355

Lhomme JP (1991) The concept of canopy resistance: historical survey and comparison of different approaches. Agric For Meteorol 54:227–240

Lindroth A, Halldin S (1986) Numerical analysis of pine forest evaporation and surface resistance. Agric For Meteorol 38: 59–79

Lynn BH, Carlson TN (1990) A stomatal resistance model illustrating plant vs. external control of transpiration. Agric For Meteorol 52:5–43

Mascart P, Taconet O, Pinty JP, Ben Mehrez M (1991) Canopy resistance formulation and its effect in mesoscale models: a HAPEX perspective. Agric For Meteorol 54:319–351

Monteith JL, Unsworth MH (1990) Principles of environmental physics, 2nd edn. Arnold, London

Mott KA, Parkhurst DF (1991) Stomatal responses to humidity in air and helox. Plant Cell and Environ 14:509–515

Price DT, Black TA (1990) Effects of short-term variation in weather on diurnal canopy CO_2 flux and evapotranspiration of a juvenile douglas-fir stand. Agric For Meteorol 50: 139–158

Ripley EA, Redmann RE (1976) Grassland. In: Monteith JL (ed) Vegetation and the atmosphere, Vol 2. Academic Press, London, p 349–398

Saugier B, Katerji N (1991) Some plant factors controlling evapotranspiration. Agric For Meteorol 54:263–277

Schulze ED, Leuning R, Kelliher FM (1995) Environmental regulation of surface conductance for evaporation from vegetation. Vegetatio 121:79–87

Segal M, Avissar R, McCumber M, Pielke RA (1988) Evaluation of vegetation effects on the generation and modification of mesoscale circulations. J Atmos Sci 45:2268–2292

Thom AS (1972) Momentum, mass and heat exchange of vegetation. Q J R Meteorol Soc 98:124–134

Thom AS (1975) Momentum, mass and heat exchange of plant communities. In: Monteith JL (ed) Vegetation and the atmosphere, Vol 1. Academic Press, London, p 57–109

Verhoef A, Allen SJ, De Bruin HAR, Jacobs CMJ, Heusinkveld BG (1996) Fluxes of carbon dioxide and water vapour from a Sahelian savanna. Agric For Meteorol 80: 231–248

Verma SB, Baldocchi DD, Anderson DE, Matt DR, Clement RJ (1986) Eddy fluxes of CO_2, water vapor, and sensible heat over a deciduous forest. Boundary Layer Meteorol 36: 71–91

Woledge J, Bunce JA, Tewson V (1989) The effect of air humidity on photosynthesis of ryegrass and white clover at three temperatures. Ann Bot 63:271–279

Editorial responsibility: Gerd Esser, Gießen, Germany

Submitted: December 5, 1997; Accepted: March 3, 1999
Proofs received from author(s): May 7, 1999